Engineering and Technology Journal

Mathematical Model of Properties and Experimental Fatigue Investigation at Elevated Temperatures of Functionally Gradient Materials

Ziadoon M.R Al-hadrayi [a b]* [iD] **, Ahmed N. Al-Khazraji** [a] [iD] **, Ahmed A. Shandookh** [a] [iD]

[a] Mechanical Engineering Dept., University of Technology-Iraq, Alsina'a street, 10066 Baghdad, Iraq.
[b] Materials Engineering Department, Faculty of Engineering, University of Kufa, Najaf, Iraq
*Corresponding author Email: me.19.31@grad.uotechnology.edu.iq

HIGHLIGHTS

- Manufacturing of functionally graded materials by the permanent casting method was studied.
- Installing and equipping a fatigue tester with a thermal chamber was employed.
- Fatigue analysis for functionally gradient materials was conducted using ANSYS at elevated temperatures.

ARTICLE INFO

ABSTRACT

Fatigue that occurs at elevated temperatures is called thermal fatigue. High temperatures and cycling loads cause thermal fatigue that can cause component failures. In this paper, induced the mathematical models for functionally gradient materials and three models of functionally gradient materials (FGMs) manufactured by permanent casting were tested to predict their thermal fatigue life. FGMs have been tested to determine the effect of fatigue and temperature interactions. FGMs models were of FGM1, FGM2, and FGM3 respectively, with the following volume fractions and gradations: [100%Al-50%Al50%Zn-50%Zn50%Al-100%Zn], [100%Al-30%Zn70%Al-70%Zn30%Al-100%Zn] and [100%Al-70%Zn30%Al-30%Zn70%Al-100%Zn]. The experimental procedure presented the mechanical properties as modulus of elasticity at two levels of temperatures (80 ℃, and 160 ℃). Through the results of the tensile test at high temperatures, it was noted that the reduction percentage was high in the second type. This was especially for the yield strength value, where the percentage reached 43% at 160 °C. In the second type, the ultimate strength was affected more at 160 °C: the decrease percentage reached 33%, and the elastic modulus at the same temperature fell by 32%. The third type is the least affected at high temperatures, as the percentage of properties decrease at 160 °C reached 16, 17, and 16% for modulus of elasticity, ultimate strength, and yield strength, respectively. Fatigue strength is the most significant among the mechanical properties, where the highest value of the fatigue limit for the third type was experimentally 149.68 MPa. While the lowest value of fatigue strength was the second type, and at the same time, on the contrary, it was less affected at high temperatures, with a rate of 8%, which reached the decrease. The simulation results from the ANSYS program regarding fatigue at high temperatures were acceptable and gave reasonable variation ratios and were very close to the experimental results.

1. Introduction

In order to provide long-term performance to structures in terms of withstanding extreme temperature gradients in specific directions while maintaining structural integrity, new classes of advanced composite materials, called functionally graded materials (FGMs), have been developed. A non-uniform distribution of the reinforcement phase provides smooth and continuous variation in properties between surfaces in this type of composite material. Material properties are gradually changed along a specific direction, eliminating corrosion, fatigue, fracture, and local stress concentration occurring as a result of abrupt changes in monolithic laminated composites[1]. In Japan, in the early 1980s, this novel concept of materials was introduced to enhance adhesion and reduce heat stress in metallurgical compounds produced for reusable missile engines [2]. Functionally Graded Materials (FGMs) were considerably progressed. Meantime, FGM principles have generated global research efforts to produce enhanced elements with superior physical characteristics in metals, ceramics, and organic compounds. Because of this recent

940

growth in composite material development, graded structures have become a new form of engineered materials. Graded materials are a relatively new class of materials with a composition and/or microstructure that differs in a single direction. Due to their continuous composition change and the absence of any specific interface, it is generally assumed that such a structure would be more resistant to thermal and mechanical cycling [3]. The essential characteristics of FGMs make them the preferred choice for almost all engineering applications. As a result of their excellent thermal and mechanical properties, FGMs are widely used in a wide range of fields in the future. In addition to aerospace and automobiles, the current application areas include energy, marine, defense, electrical/electronics, and thermoelectric. Functionally graded materials have a wide range of applications, and some parts are suitable for aerospace applications. A functionally graded material consisting of 25% aluminum and 25% copper has been manufactured. Researchers examined the effects of Al₂Cu variations on thick-walled functionally graded (FG) cylindrical shells. High-entropy FG composite is obtained by centrifugally casting an Al-25 wt.% Cu hypo-eutectic alloy ingot [4]. Several FGMs components are suitable for automotive applications. Investigated functionally graded Al/Mg and Al/Al 7075 composites manufactured by die casting. FGMs made with combinations of Al/Mg and Al/Al 7075 are characterized. An attempt has been made to produce FGMs using gravity casting. A microstructure and mechanical property analysis is performed after the FGMs are manufactured. In microhardness tests and microscopic observations, a continuous gradient FGM was observed between metal Al/Mg and metal Al 7075 [5].

Examined the analysis of magnetically modified hypereutectic functionally graded aluminum composites. Vertical centrifugal casting was used to produce functionally graded aluminum metal matrix composites (FGAMMCs). Casting centrifugally has been proven to be a versatile casting method for producing various types of FGM components based on their properties.[6]. The use of functionally graded materials (FGMs), containing ceramic and metallic constituents, is widespread in high-temperature applications. The powder technology technique was used to design and fabricate six sets of FGMs samples [7]. A method of centrifuging an alloy (Al-TiO₂) to produce thick hollow functionally graded cylinders. This objective was accomplished by designing and manufacturing a vertical centrifugal casting machine. Through FG cylinder preparation, linear and graded hardness were demonstrated across a wide range of thicknesses [8]. The layers in the epoxy matrix were composed of functionally graded polymer nanocomposites composed of silica (SiO2) nanoparticles (14-36 nm in diameter) distributed throughout ultrasonication by hand lay-up. Using this method, the nanoparticles were graded in terms of their volume fraction (V_f.) [9]. An epoxy matrix was mixed with Alumina (Al₂O₃) nanoparticles (50 to 100 nm) through five layers of 1.2 mm thickness per layer to produce a functionally graded polymer nanocomposite (FGPNC). In order to manufacture the graded composite sheet, different percentages of the nanoparticles were taken and cast in acrylic molds [10]. Those materials that are subject to rapid temperature changes, such as high-pressure die casting and hot forging, have a high level of thermal fatigue resistance. This study therefore aimed to investigate the suitability of thermal fatigue-resistant functionally graded materials (FGMs).

This study investigated the use of FGM in permanent castings that are subjected to thermal fatigue and determined which combination of materials would provide the best results. As a result of this study, further testing will be undertaken, and the knowledge gained will be highly useful in the industrial environment, further reducing the costs related to permanent casting repair.

2. Research procedures

The research consists of two parts. The first part deals with the formulation of mathematical models for FGMs, preparing samples and experimental tests for mechanical properties, and fatigue testing. In addition, the effect of high temperatures on properties in general. The second part is through the finite element method using the ANSYS program.

2.1 Mathematical models formulation for FGMs

Despite being exceedingly heterogeneous, the FGM's mechanical characteristics progressively change over time between different surfaces. An effective study of FGMS requires a more complete understanding of its complicated asymmetric morphology. This formulation can establish mathematical models and identify issues, enhancing numerical techniques for structures with FGM as part of their constituent structure. FG structures provide the capability of determining how materials are conveyed at different spatial levels. The ability to determine the transport of materials at various spatial levels is a crucial feature of the FG structure. Specialized composite materials known as FGMs are composed of several constituent stages that are provided according to established guidelines [11].

Typically, when the thickness varies, the material's characteristics tend to vary rapidly. The common method for describing FGMs is to use different mathematical idealizations. The most prevalent models in the static and dynamic analysis are the ones listed below.

2.1.1 Power law

The volume fraction of the material and its physical characteristics vary along the thickness direction. FGM designs require material (A) on one of the outer surfaces and material (B) on the other. Plates and beams are both characterized by the various FGMs. Based on the power-law distribution shown below, it is possible to determine the Material (A) volume fraction (V_A) for the FGMs as [12]:

$$V_A(z) = \left(\frac{z+\frac{h}{2}}{h}\right)^k \qquad (1)$$

The formula for the volume fraction total of the two materials is:

$$V_A(z) + V_B(z) = 1 \tag{2}$$

Where V_A is the volume fraction of material (A), V_B is the volume fraction of material (B), k is the variation index of a power law and is a variable parameter that is not negative, where k [0,∞). A fully material (A) plate is represented by the value of k=0, whereas a fully material (B) plate is shown by k=∞. It is supposed that the material structure of the top surface (z=h/2) is rich in material (A), and that it continually differs from the surface of the bottom surface (z=h/2) which is rich in material (B). A cartesian coordinate system (x, y, z) is used on the plate's middle surface to describe the plate's motion. X and Y represent the in-plane coordinates, while z represents the out-of-plane. The FG plate's material property is determined by[12]:

$$P(z) = (P_A - P_B)(\frac{z+\frac{h}{2}}{h})^k + P_B \tag{3}$$

$$E(z) = (E_A - E_B)(\frac{z+\frac{h}{2}}{h})^k + E_B \tag{4}$$

Where, P_A, P_B, the materials properties values of material (A) and (B), a description of the FG plate's constituents or beam, respectively. In this study, material (A) is Aluminum alloys, and material (B) is zinc alloys.

2.1.2 The exponential law

Numerous related research, including those in the following, use the exponential function to describe the material characteristics of FG plates, as below [13]:

$$E(z) = E_t e^{(-ß(1-\frac{2z}{h}))}, ß = \frac{1}{2}ln(\frac{E_t}{E_b}) \tag{5}$$

$$\lambda(z) = \lambda_B e^{(zln\frac{\lambda_A}{\lambda_B})}, \alpha(z) = \alpha_B e^{(zln\frac{\alpha_A}{\alpha_B})} \tag{6}$$

Where, E_t and E_b are the top and bottom elasticity moduli of the beam, respectively. A plate or beam made from FGM with a thickness (h) will have an elasticity modulus $E(z)$. $\lambda(z)$ and $\alpha(z)$ are the thermal conductivity and thermal expansion of the FGMs plate or beam, respectively. A plot of Young's modulus versus plate thickness.

2.1.3 Sigmoid law

FGMs structures and their variations in thickness are not well described by low-power functions. Due to the continuous nature of material attributes in an FG part, stresses accumulate at the interface. A power index is used to address this problem since the transition between material attributes is not smooth. The following two formulae demonstrate power-law gradients and how they relate to volume fraction [14]:

$$V_1(z) = 1 - \frac{1}{2}(\frac{\frac{h}{2}-z}{\frac{h}{2}})^k \; ; \; (0 \leq z \leq \frac{h}{2}) \tag{7a}$$

$$V_2(z) = \frac{1}{2}(\frac{\frac{h}{2}-z}{\frac{h}{2}})^k \; ; \; (-\frac{h}{2} \leq z \leq 0) \tag{7b}$$

A sigmoid formula can be used to estimate the value of the elastic modulus of the FGM based on the rule of mixture:

$$E(z) = V_1(z)E_1 + [1 - V_1(z)]E_2 \; ; \; (0 \leq z \leq \frac{h}{2}) \tag{8a}$$

$$E(z) = V_2(z)E_1 + [1 - V_2(z)]E_2 \; ; \; (-\frac{h}{2} \leq z \leq 0) \tag{8b}$$

2.2 Experimental Procedure

2.2.1 Samples

A functionally graded aluminum-zinc alloy was fabricated from materials available on the local market for this work. A cast iron mold with dimensions of (21 cm) in length and (2 cm) in diameter was used for manufacturing. To avoid the disadvantages of casting, all samples were annealed after manufacturing three models with different weight ratios. Specimens were shaped according to standard dimensions and according to ASTM standards. As shown in Table 1, each alloy was examined for its chemical components (spectrophotometer).

As shown in Figure 1, the flow chart illustrates how functionally graded materials are manufactured. The process begins with the fractional volume and iron mold, followed by smelting the ingots in a furnace before pouring molten metal into the iron mold. presents the mechanical properties of the alloys used in the manufacturing of functionally graded material .As shown in Table 2.

Table 1: Chemical compositions of alloys [15]

Alloys	Si%	Fe %	Cu%	Mn %	Mg %	Cr%	Ni%	Zn %	Ti%	P%	Pb%	Al %
Al alloys	0.166	0.625	0.0878	0.00058	0.00012	0.0214	0.00093	0.017	0.0307	0.00015	0.00036	99
	Al %	Mg %	Cu%	Fe%	Pb%	Cd%	Sn%	Ni %	Zn%			
Zn alloys	3.8	0.03	0.25	0.1	0.005	0.004	0.003	-	95.8			
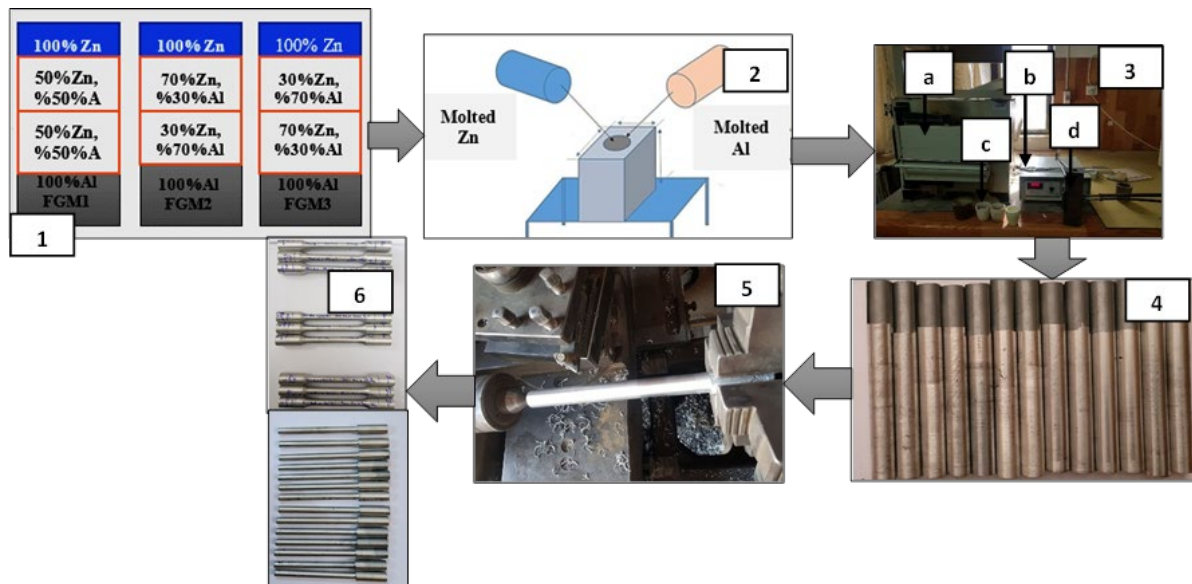
Figure 1: Flowchart of FGMs preparation 1) Scheme of volume fraction of FGMs 2) Scheme of casting process 3) casting process; a)Furnace; b) temperature controller; c) melting pots; d) Iron mold 4) samples 5) turning operation 6) ASTM samples for testing.

Table 2: Materials' mechanical properties[15]

Alloys	Elastic modulus (GPa)	Ultimate Strength (MPa)	Yield Strength (MPa)	Density (Mg/m³)	Poisson's ratio	Melting Temperature (°C)
A	70.5±2	340±5	265±5	2.66±0.2	0.33	640±5
Zn	85±2	320±5	225±5	7.14±0.2	0.25	422±5

2.2.2 Tensile test

Tensile tests were conducted on the WDW-100E universal testing machine as shown in Figure 2 (a). In the tests the crosshead speed was 0.1 mm/min and the ASTM E8M [16]was used. Stress-strain curves can be calculated by dividing tensile stress on strains into different strain values based on the type of FGMs being used, and then the tensile test was performed at elevated temperatures. To heat the chamber covering the gauge length of the sample, a temperature sensor and a thermocouple are used as shown in figure 2 (b). A digital monitor shows the temperature of the heating chamber on the control box, which is connected to the heating chamber, as shown in figure 2 (b). At these temperatures, 80 degrees Celsius, and 160 degrees Celsius, the heating chamber is heated at two levels. Further, the room temperature is taken into account.
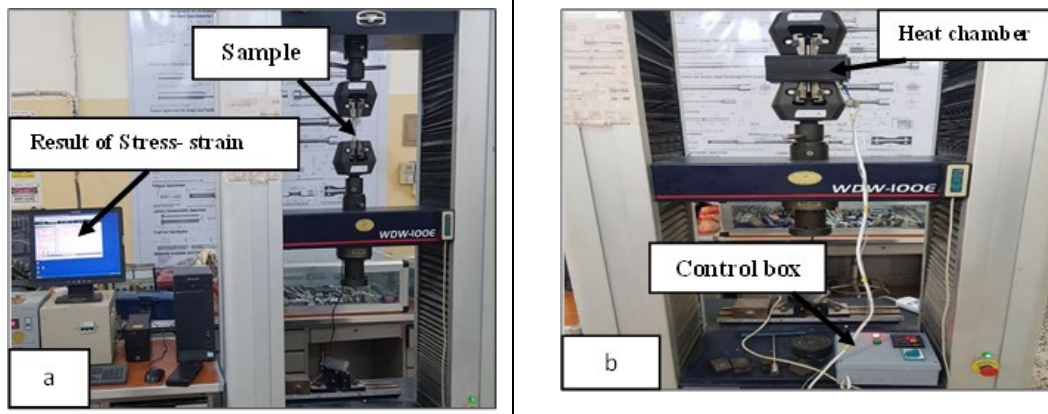
Figure 2: Tensile test a) at room temperature b) at elevated temperature

2.2.3 Fatigue test

For the study of fatigue, thermal fatigue, and creep-fatigue interactions of solids, Figure 3 illustrates a rotating bending fatigue test machine. The machine features a rotating motor with 3000 RPM The parts indicated in the figure are the assembled components of this test device.
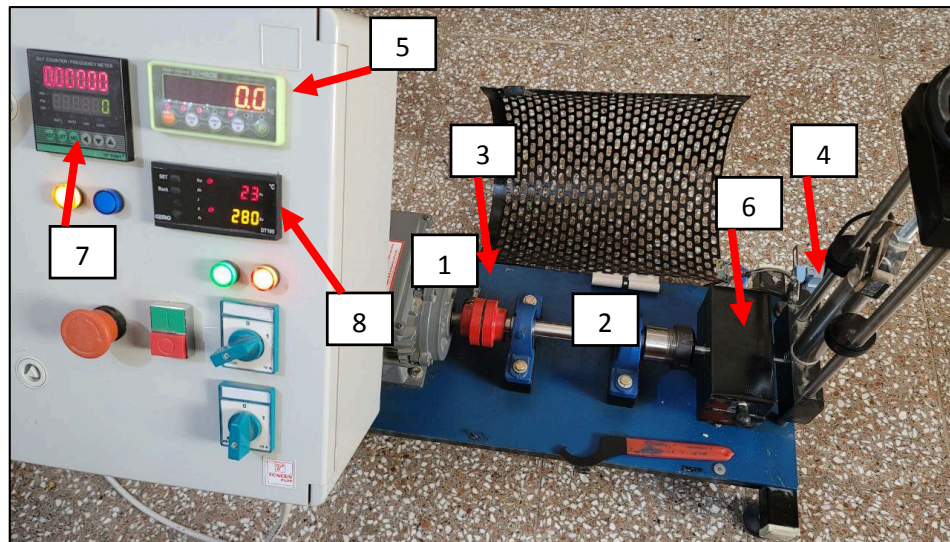
Figure 3: Machine of test for fatigue, thermal fatigue, and creep-fatigue interaction 1) a rotating motor; 2) two supporting bearings; 3) Proximity laser sensor; 4) a limit switch; 5) a digital loading system; 6) a cast iron furnace with a thermally insulating coating; 7) a digital counter; 8) a temperature controller digital.

With a constant frequency of 50Hz, a rotating sample was clamped and loaded with up to 1 KN of concentrated force. An experiment was conducted with a sinusoidal cyclic load applied at a stress ratio R = -1 (minimum load/maximum load). Cylindrical samples were subjected to alternate bending stresses after a given number of load cycles. The thermal fatigue behaviour of FGMs will be represented as an S-N curve. Based on bending moment values, equation (12) calculates alternating bending stress. The stress ratio (R) can be calculated using constant amplitude loads as follows [17]:

$$R = \frac{\sigma_{min.}}{\sigma_{max.}} \quad \text{(For reversed bending, R= -1)} \tag{9}$$

In order to calculate the bending moment (M_b) for the load and lever arm, the following formula was used for the solid sample:

$$M_b = F.a \tag{10}$$

$$I_b = \frac{\pi\, d^3}{32} \tag{11}$$

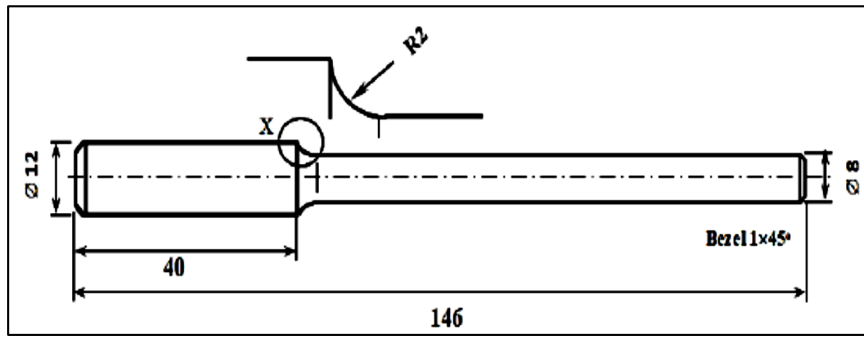A sample of FGM as an ASTM standard is shown in figure 4.

Figure 4: Fatigue sample based on ASTM [18]

Calculating the alternating stress amplitude can be achieved by taking the sectional modulus I_b of the sample into account. After substituting the values of the diameter and arm length defined later, the equation becomes:

$$\sigma_a = \frac{M_b}{I_b} = \frac{32\ F.a}{\pi\ d^3} \cong 2\ F \tag{12}$$

Where, F is applied force (N), a is the bending arm length (mm), d is the diameter of the sample (mm), and σ_a is the alternative stress (MPa). Equation (12) appears in this form, equivalent to approximately twice the applied force, after substituting for the value of the bending moment arm length and the sample diameter of 106 mm and 7.9 mm, respectively.

Thermal-Fatigue data is illustrated graphically with a stress-life curve. A fatigue life function represents alternating stress amplitudes and cycles to failure[19]. The Basquin relation, for finite lives (high cycle fatigue), is often used to express S-N curves analytically. It is possible to predict life without having much information about a material by using the Basquin curve this way[17]:

$$\sigma_a = A\ N_f^B \quad (MPa) \tag{13}$$

Where A and B are constants determined experimentally, N_f is the number of cycles to failure.

In order to find out the behavior of functionally graded materials under the influence of fatigue, a test was conducted on a sample of the three models of functionally graded materials at room temperature under the influence of six levels of loads.

In addition, to find out the behavior of functionally graded materials under the influence of fatigue at elevated temperatures, the test was conducted for the three models at 80 and 160 °C. Table 3 contains full details of the mechanical properties that entered into the fatigue test.

Table 3: Loads and stresses applied to the fatigue test

Temp. °C	$\frac{\sigma_a}{\sigma_y}$	FGM 1			FGM 2			FGM 3		
		F (N)	σ_a (Mpa)	σ_y (Mpa)	F (N)	σ_a (Mpa)	σ_y (Mpa)	F (N)	σ_a (Mpa)	σ_y (Mpa)
	1.4	175	350	242	161	322	230	182	364	260
	1.2	150	300	242	138	276	230	156	312	260
25	0.9	108.9	217.8	242	103.5	207	230	117	234	260
	0.8	100	200	242	92	184	230	104	208	260
	0.6	75	150	242	69	138	230	78	156	260
	0.4	50	100	242	46	92	230	52	104	260
	1.4	151.2	302.4	216	131.6	263.2	188	171.5	343	245
	1.2	129.6	259.2	216	112.8	225.6	188	147	294	245
80	0.9	97.2	194.4	216	84.6	169.2	188	110.2	220.5	245
	0.8	86.4	172.8	216	75.2	150.4	188	98	196	245
	0.6	64.8	129.6	216	56.4	112.8	188	73.5	147	245
	0.4	43.2	86.4	216	37.6	75.2	188	49	98	245
	1.4	139.3	278.6	199	92.4	184.8	132	152.6	305.2	218
	1.2	119.4	238.8	199	79.2	158.4	132	130.8	261.6	218
160	0.9	89.5	179.1	199	59.4	118.8	132	98.1	196.2	218
	0.8	79.6	159.2	199	52.8	105.6	132	87.2	174.4	218
	0.6	59.7	119.4	199	39.6	79.2	132	65.4	130.8	218
	0.4	39.8	79.6	199	26.4	52.8	132	43.6	87.2	218

2.3 Finite Element Analysis (FEA)

Finite element analysis (FEA) is useful for simulating various analyses and solving mechanical problems, including fatigue, creep, and structural problems. ANSYS was used to analyze fatigue in functionally gradient materials at elevated temperatures. Solid hexahedra (solid187) were used to construct the elements, which had 20 nodes each. A stress life model was developed based on reverse bending experiments and the mechanical properties of the selected material (modulus of elasticity, yield stress, tensile strength, temperature, etc.). A mesh of elements was generated based on the model geometry in Figures 5 a and b. A bending load was generated with boundary conditions as shown in Figures 5 c and d.
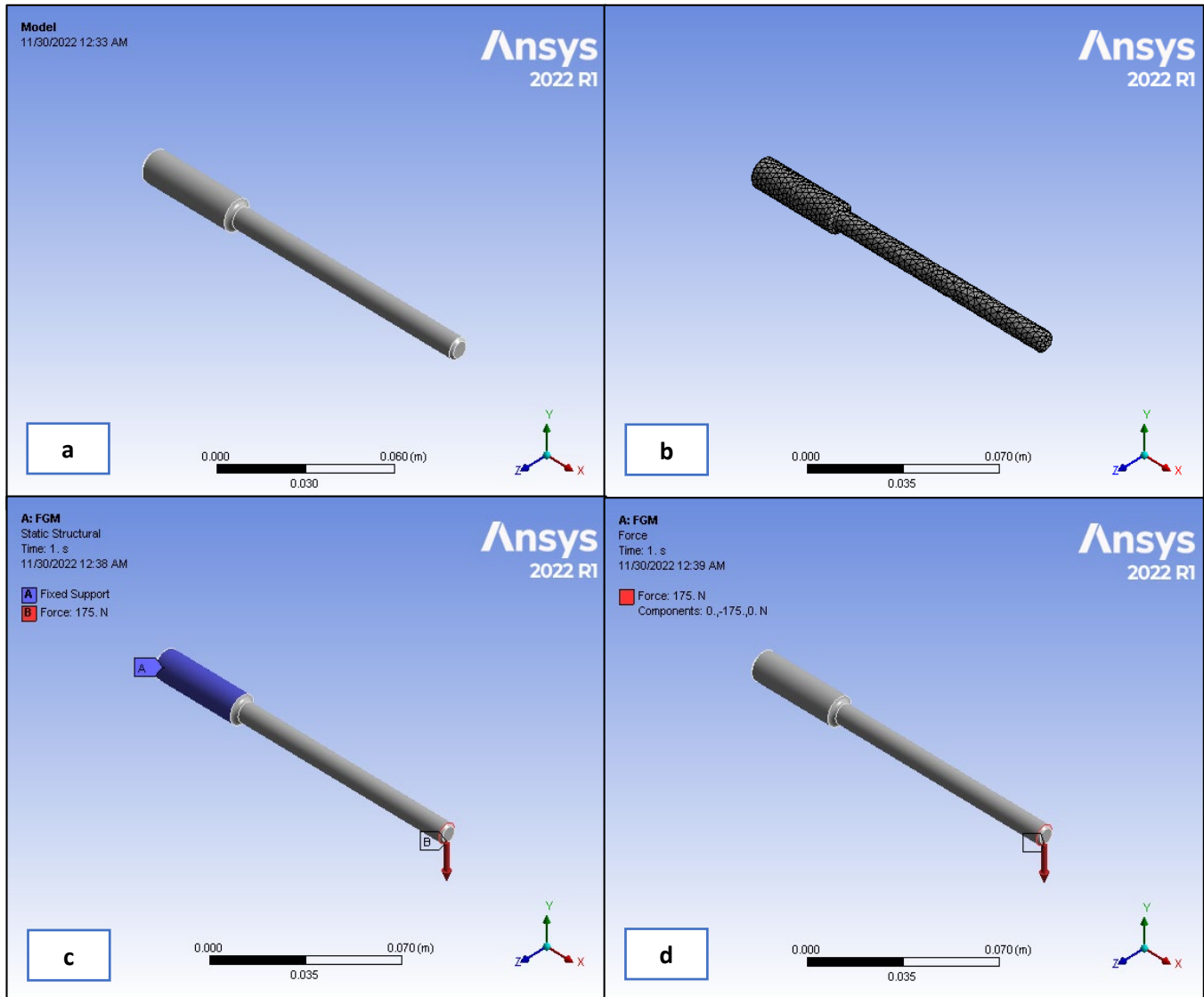
Figure 5: The approach to stress life model a) Geometry model b) Mesh c) Boundary condition d) Bending loading

3. Results and Discussion

3.1 Mathematical models

Upper and lower surfaces have different effective material properties, such as Young's modulus, Poisson's ratio, coefficients of thermal expansion, thermal conductivity, etc. Poisson's ratio and Young's modulus of the beam, however, vary continuously only in the thickness direction (z-axis), i.e., $E = E(z)$, $\rho = \rho(z)$. Through the thickness direction, Young's modulus of FGM plates varies with power-law functions (P-FGM), exponential functions (E-FGM), or sigmoid functions (S-FGM). A mixture of these two materials makes up the through-thickness property. Figure 6 presented the results of the elastic modulus of the functionally graded material with the change in the value of K based on power law. The value of the properties of the elastic modulus of the aluminum alloy and the zinc alloy was calculated by considering the functionally graded material metal-metal. Figure 7 presented the density property of aluminum and zinc with different power law k.
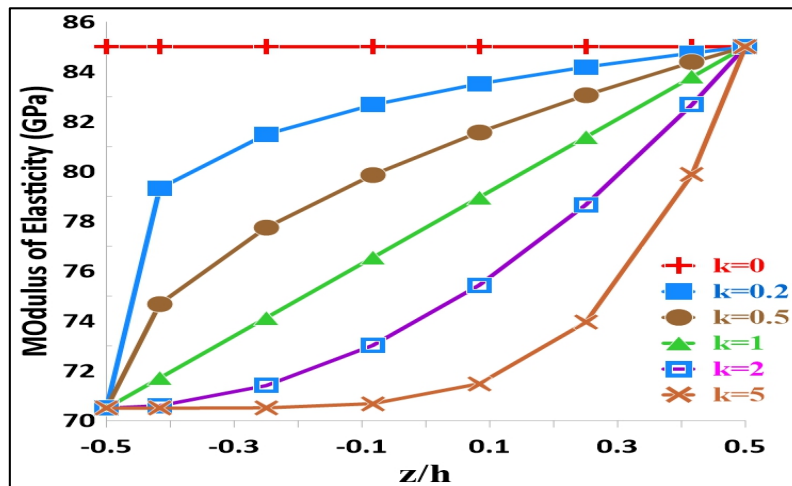
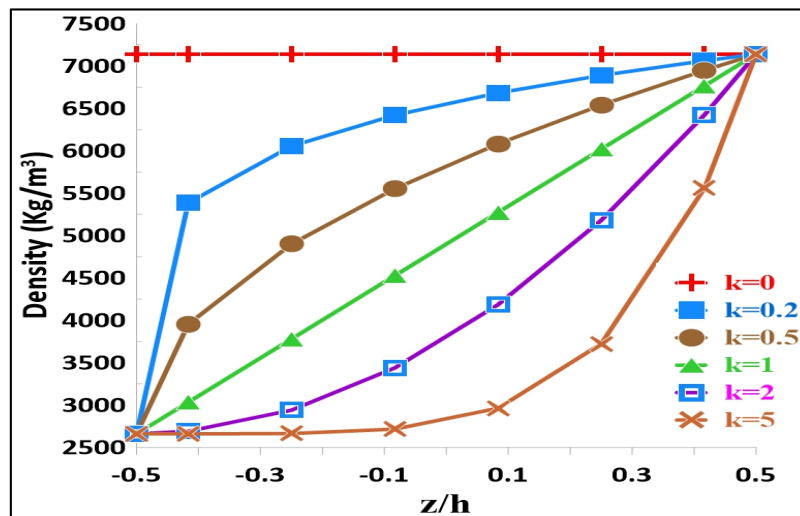**Figure 6:** P-FGM with k and variations of Young's modulus

Figure 7: P-FGM with k and variations of densities

While Figures 8 and 9 presented the results of the solutions of the Sigmoid and Exponential equations, respectively, in terms of the distribution of the modulus of elasticity for aluminum and zinc with different power K and thickness.

Where the exponential law was approximately linear. Figure 8 illustrates the variation in Young's modulus in the thickness direction of the S-FGM plate shows that Young's modulus is gradual due to the combination of two power law functions.
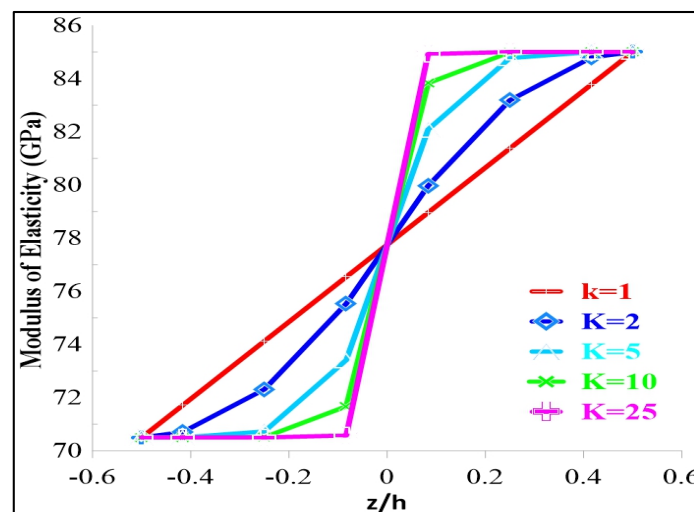

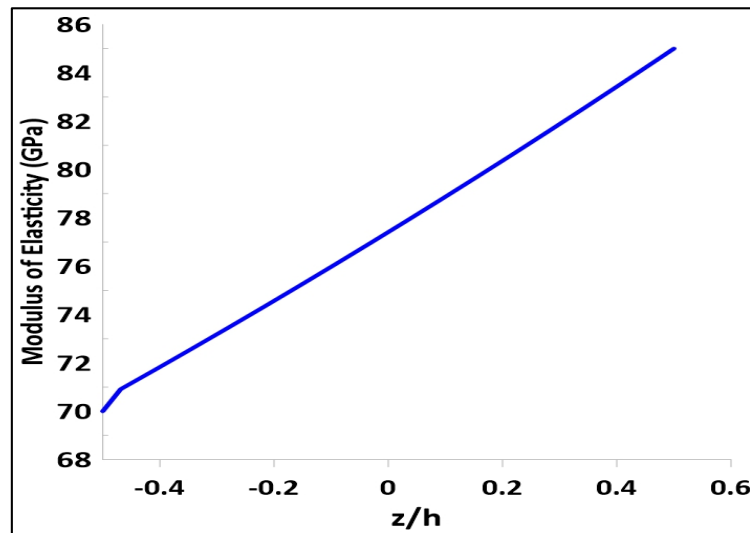**Figure 8:** S-FGM with different k and variation of Young's modulus

Figure 9: E-FGM with different k and variation of Young's modulus

It is clear from the results that the properties change as the upper layer progresses down to the lower layer, i.e. the thickness of the aluminum alloy is thicker than the thickness of the zinc alloy, and therefore the effect of the P value is clearly evident, since the larger the change, the greater the change in the properties and with the thickness of the layers, and this is the mark of functionally graded materials so that the properties of the material can be known through these three laws.

3.2 Tensile at elevated temperatures

Figure 10 shows the stress-strain behaviour of alloys and FGMs for the three manufactured models. In contrast with the alloys from which it was made, FGM has a different stress–strain curve. Comparing the FGM with the original alloys, it had the best elastic modulus and showed 79 GPa at its highest value, the highest value of the elastic modulus among the alloys. Table 4 shows the values of the results of the elastic modulus, ultimate strength, and yield strength at elevated temperatures. Where it was observed that the first and second types were affected more than the third type of functionally graded materials. Additionally, the ultimate stress of the third type of FGM was 377 MPa; tensile strength of model FGM 3 is 6% and 10% higher than that of versions FGM 1 and 2, respectively. As compared to aluminium–zinc alloys, the strength was improved by 22% on average. It also presented the behavior of functionally graded materials at high temperatures, which greatly affected the modulus of elasticity, as well as the tensile strength can be observed through the stress-strain curves. The modulus of elasticity of the first type of functionally graded materials decreased by 7% at the temperature of 80 °C, The percentage reached 20% at 160°C. As for the second model of functionally graded materials, the elasticity modulus decreased by 12% at the temperature of 80 °C and by 32% at the temperature of 160 °C. While the third type of functionally graded materials had the least effect on their behavior at high temperatures, as it decreased by 6% at a temperature of 80 °C and by 16% at a temperature of 160 °C. The difference in susceptibility at high temperatures is due to the influence of the mixing ratios and the manufacturing method for the functionally graded materials. Therefore, the results appeared different and with different curves and influences for each type. The results showed that the third model is the best type in the manufactured functional graded materials.

Table 4: Values of elastic modulus, ultimate strength, and yield strength.

Temp. ºC	FGM 1			FGM 2			FGM 3		
	E (Gpa)	σ_u (Mpa)	σ_y (Mpa)	E (Gpa)	σ_u (Mpa)	σ_y (Mpa)	E (Gpa)	σ_u (Mpa)	σ_y (Mpa)
Room temp.	77	355	242	74	344	230	79	377	260
80	72	322	216	65	288	188	74	340	245
160	62	302	199	50	229	132	66	310	218
Decrease Percentage % at 80	6	9	11	12	16	18	6	10	6
Decrease Percentage% at 160	19	15	18	32	33	43	16	17	16

The reason for the effect of the second type of functionally graded materials is the mixing ratios. These ratios were symmetrical as they are with the first type, which showed less effect. While the third type had a somewhat slight effect, and this is due to the inconsistency in the mixing ratio between aluminum and zinc.
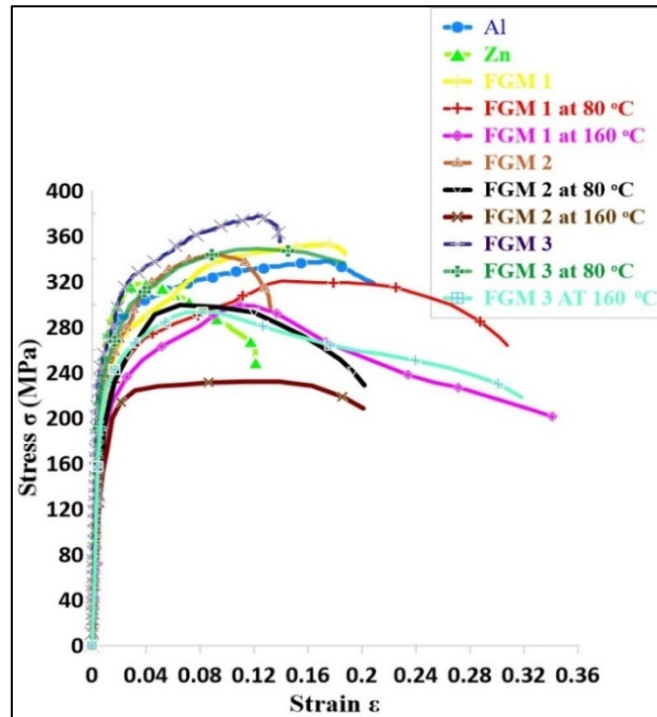
Figure 10: Tensile results at high temperatures

3.3 Fatigue results (Experimental and Numerical)

In Figure 11, the numerical and experimental results are presented at room temperature. Based on the above-mentioned equations, alternating applied stresses were calculated as a cycle to failure in the form of a curve. It has been noted that functionally graded materials, especially metals, have received little research attention in fatigue. A S-N curve was drawn for three models that were represented experimentally and numerically. The third type of material has been observed to fail after more than one million and two hundred thousand cycles. During the manufacturing process, the materials were mixed in different ratios, which led to this effect and a difference in the number of cycles. In the experiment, the alternating stress ratio was 1.4 to 0.4 of yield strength. In addition, these ratios have been applied at elevated temperatures.
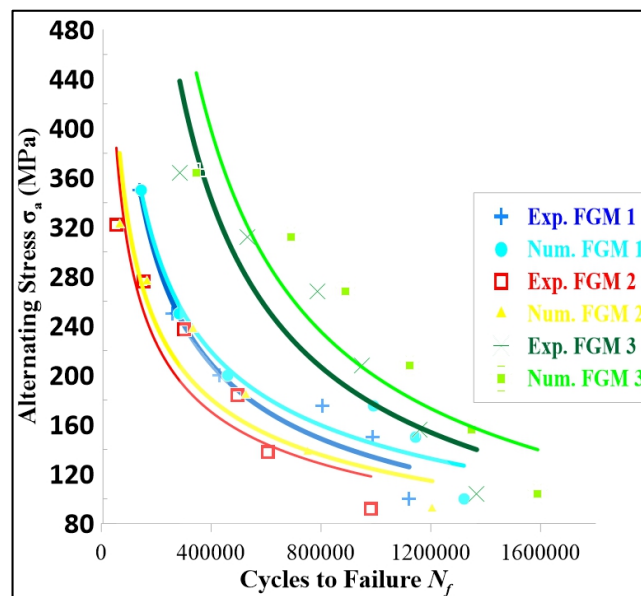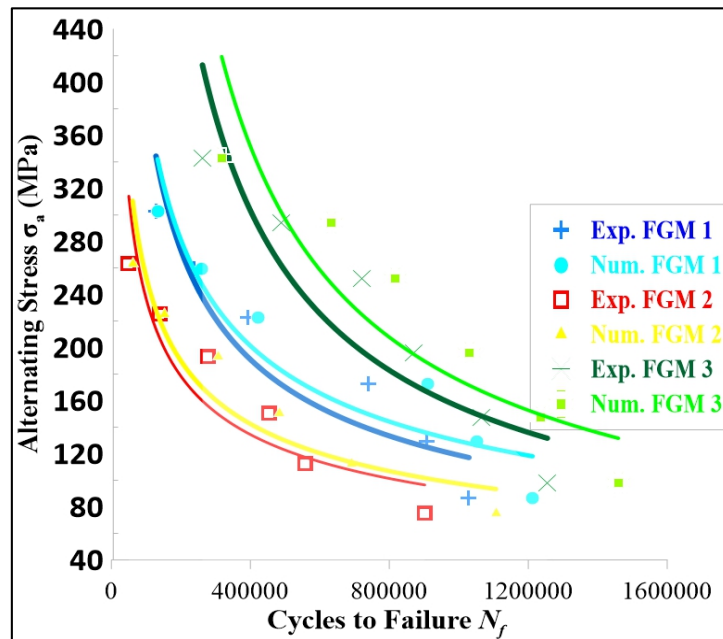

Figure 11: S-N curves of three models for FGMs are investigated experimentally and numerically at room temperature

A range of cumulative thermal fatigue tests is conducted at low to high stress levels as temperatures increase from room temperature to 80 and 160 °C. The validity of the above equation was checked using three different temperature ranges. Figure

12 represented the s-n curves of three models for FGMs at 80 ºC. The results were also experimentally and numerically determined. In addition,, Figure 13 represented the s-n curves of three models for FGMs at 160 ºC. The results were also experimentally and numerically determined.

Figure 12: S-N curves of three models for FGMs are investigated experimentally and numerically at 80 ºC

It was observed through the results represented by S-N curves that the fatigue strength of the third type is stronger than the first and second types, and this is due to the mixing ratios of the functionally graded material. In both of the first and second types, the proportions of aluminum and zinc are symmetrical in the samples, and the zinc is sensitive to high temperatures and its behavior, which leads to the weakness of the sample and then leads to an accelerated fracture. While the third type, the mixing proportions were opposite for aluminum with zinc, and this gives sufficient plasticity and ductile behavior to the material and then fracture.
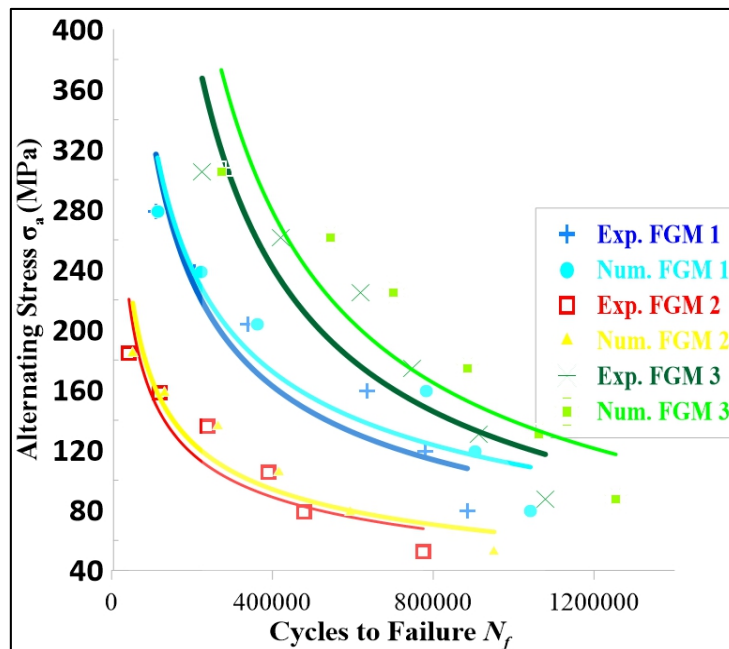
Figure 13: S-N curves of three models for FGMs are investigated experimentally and numerically at 160 ºC

The reason behind this phenomenon is the activation of damage micro mechanisms by high temperature testing, which combine with fatigue damage to dramatically reduce fatigue life. As shown in Figures (11-13), increasing the temperature results

in an increased damage ratio and cyclic ratio, which accelerates fracture acceleration. It was observed in Table 5 that cycles to failure were not only affected by temperature, but also by load sequences, e.g. (Low-High) stress sequence loading at a defined temperature. It is difficult to treat thermal damage and fatigue damage separately in fracture failure when the metal is exposed to high temperatures. There is a significant reduction in the number of cycles in high temperature conditions due to the interaction between temperature and fatigue. The reduction life ratio increases with temperature as shown in Tables 6 and 7. Changing the temperature will increase in the damage ratio and cyclic ratio as shown in Table 8.

Table 5: Equations of fatigue life for three models of FGMs at room temperature

Material	Fatigue life equation (Exp.)	Fatigue life equation (Num.)	Fatigue limit (Exp.) (MPa)	Fatigue limit (Num.) (MPa)	Disparity %
FGM1	$\sigma = 121343\, N_f^{-0.493}$	$\sigma = 80792\, N_f^{-0.458}$	133.66	144.34	7.4
FGM2	$\sigma = 28561\, N_f^{-0.398}$	$\sigma = 30631\, N_f^{-0.399}$	116.89	123.64	5.45
FGM3	$\sigma = 3*10^6\, N_f^{0.717}$	$\sigma = 5*10^6\, N_f^{-0.747}$	149.68	164.8	9.1

Table 6: Equations of fatigue life for three models of FGMs at 80 °C

Material	Fatigue life equation (Exp.)	Fatigue life equation (Num.)	Fatigue limit (Exp.) (MPa)	Fatigue limit (Num.) (MPa)	Disparity %
FGM1	$\sigma = 116325.94\, N_f^{-0.4932}$	$\sigma = 77685.79\, N_f^{-0.45811}$	127.78	138.573	7.788
FGM2	$\sigma = 27605.366\, N_f^{-0.3976}$	$\sigma = 29603.943\, N_f^{-0.39865}$	113.604	120.157	5.45
FGM3	$\sigma = 2921461.2\, N_f^{0.7173}$	$\sigma = 4959182.3\, N_f^{-0.747081}$	145.144	163.276	11.1

Table 7: Equations of fatigue life for three models of FGMs at 160 °C

Material	Fatigue life equation (Exp.)	Fatigue life equation (Num.)	Fatigue limit (Exp.) (MPa)	Fatigue limit (Num.) (MPa)	Disparity %
FGM1	$\sigma = 107953.49\, N_f^{-0.4932}$	$\sigma = 72478.453\, N_f^{-0.458106}$	118.58	129.292	8.285
FGM2	$\sigma = 25991.354\, N_f^{-0.3969}$	$\sigma = 27869.637\, N_f^{-0.3978}$	108	114.375	5.573
FGM3	$\sigma = 2620767.4\, N_f^{0.71693}$	$\sigma = 4428695.5\, N_f^{-0.74699}$	130.87	145.99	10.35

Table 8: Results of thermomechanical fatigue damage

Material	FGM 1	FGM 2	FGM 3
Fatigue limit at room temperature (Exp.)	133.66	116.89	149.68
Fatigue limit at 80 °C (Exp.)	127.78	113.604	145.144
Fatigue limit at 160 °C (Exp.)	118.58	108	130.87
Damage $= \frac{\sigma_T}{\sigma_r}$	0.956	0.971	0.969
Damage $= \frac{\sigma_T}{\sigma_r}$	0.887	0.923	0.874
Decrease Percentage at 80 °C %	4	3	3
Decrease Percentage at 160 °C %	11	8	12

Where σ_T, σ_r, are the strength at elevated temperatures, and the strength at room temperature, respectively.

4. Conclusion

It enhances numerical techniques for structures that have FGM as a constituent structure through the establishment of mathematical models and identification of issues. Structures of FG can provide an understanding of how materials are conveyed over different spatial scales. In three types and mixing ratios, functionally graded materials were cast with the permanent casting method. two levels of temperature were applied to these samples of tensile test, (80 and 60 °C). Heating chambers consist of heating chambers and sensors connected to control boxes that control the temperature. Stress-strain curves were used to demonstrate the behavior of the functionally graded material under high temperatures. Functionally gradient materials were studied under rotating bending and range temperatures for their thermal-fatigue properties. It can be summarized in the following points:

1. The properties of the functionally graded materials were represented by the three governing laws (power law, exponential law, and sigmoid law), and the results demonstrated a good representation for determining the properties of any material and its relationship to the thickness required in the case of aluminum and zinc. Also, the effect of P on the change in properties.

2. Testing was conducted on three types of functionally graded materials, and the results indicated that the third type was the best. The values for the properties were (79 Pa, 377 MPa, and 260 MPa), Young's modulus, ultimate strength, and yield strength, respectively.
3. Tensile test at two levels of high temperature (80 and 160 °C) for the three models of functionally graded materials, where the results showed the behavior of these materials and the amount of affected that occurred to them, which was slightly affected at 160 °C for the third type, which was at a rate of (16,17,16 %) for modulus of elasticity, ultimate strength, and yield strength, respectively. The results showed a significant effect of the second type, which was (32,33,43%) for the modulus of elasticity, ultimate strength, and yield strength, respectively.
4. The fatigue test was experimentally and simulated for three types of functionally graded materials. The results showed that the best material is the third type, as its fatigue strength is 149.68 MPa. The experimental work was verified by simulation, and the disparity ratios showed acceptable rates. In addition, the fatigue test was conducted at two levels of elevated temperature (80 and 160 °C) and showed the behavior of the functionally graded material at elevated temperature. The experimental and simulation results showed a slight effect for the third type, on the contrary, for the first and second types.

Acknowledgment

Author Contribution

The work was equally contributed by all authors.

Funding

Data Availability Statement

A copy of the data supporting the findings of this study can be obtained from the corresponding author upon request.

Conflicts of Interest

The authors declare that there is no conflict of interest.

References

[1] B. Kieback, A. Neubrand, H. Riedel, Processing techniques for functionally graded materials, Mater. Sci. Eng. A., 362 (2003) 81–106. https://doi.org/10.1016/S0921-5093(03)00578-1

[2] M. Koizumi , M. Niino, Overview of FGM research in Japan, Mrs Bull., 20 (1995) 19–21. https://doi.org/10.1557/S0883769400048867

[3] A. Mortensen , S. Suresh, Functionally graded metals and metal-ceramic composites: Part 1 Processing, Int. Mater. Rev., 40(1995) 239–265. https://doi.org/10.1179/imr.1995.40.6.239

[4] A. Mehditabar, G. H. Rahimi, S. E. Vahdat, Mechanical properties of Al 25 wt.% Cu functionally graded material, Sci. Eng. Compos. Mater., 26 (2019) 327–337. https://doi.org/10.1515/secm-2019-0014

[5] G. Mondal, P. K. Rout, G. Mohanty, B. Surekha, Characterization and Comparison of Functionally Graded Al/Mg and Al/Al 7075 Metal Matrix Composites Manufactured by Die Casting, Adv. Man. Tec. Spr., (2019) 193–198. https://doi.org/10.1007/978-981-13-6374-0_23

[6] T. Varghese, T. P. D. Rajan, B. C. Pai, Reciprocating wear analysis of magnesium-modified hyper-eutectic functionally graded aluminium composites, Trans. Indian Inst. Met., 72 (2019) 1643–1649. http://dx.doi.org/10.1007/s12666-019-01706-z

[7] A. A. Atiyah, Fabrication, Characterization and Modeling of Al2o3/Ni Functionally Graded Materials, Eng. Tech. J., 32 (2014) 2302 -2286 . http://dx.doi.org/10.30684/etj.32.9A15

[8] A. H. Ataiwi, A. A. Atiyah, M. A. Madhloom, Mechanical Characteristics of Prepared Functionally Graded Cylinder by Centrifugal Casting, Eng. Tech. J., 32 (2014).

[9] M. M. S. Shareef, A. N. Al-Khazraji, S. A. Amin, Flexural Properties of Functionally Graded Silica Nanoparticles, IOP Conf. Ser. Mat. Sci. Eng., 1094 (2021) 012174. http://dx.doi.org/10.1088/1757-899X/1094/1/012174

[10] M. Shareef, A. N. Al-Khazraji, S. A. Amin, Flexural Properties of Functionally Graded Polymer Alumina Nanoparticles, Eng. Tec. J., 39 (2021) 821–835. http://dx.doi.org/10.30684/ETJ.V39I5A.1949

[11] S. K. Sah , A. Ghosh, Influence of porosity distribution on free vibration and buckling analysis of multi-directional functionally graded sandwich plates, Compos. Struct., 279 (2022) 114795. https://doi.org/10.1016/j.compstruct.2021.114795

[12] E. K. Njim, S. H. Bakhy, M. Al-Waily, Analytical and numerical investigation of buckling behavior of functionally graded sandwich plate with porous core, J. Appl. Sci. Eng., 25 (2021) 339–347. https://doi.org/10.6180/jase.202204_25(2).0010

[13] K. S. K. Reddy, T. Kant, Three-dimensional elasticity solution for free vibrations of exponentially graded plates, J. Eng. Mech., 140 (2014) 4014047. https://doi.org/10.1061/(ASCE)EM.1943-7889.0000756

[14] S. Nikbakht, S. Kamarian, M. Shakeri, A review on optimization of composite structures Part II: Functionally graded materials, Compos. Struct., 214 (2019) 83–102. https://doi.org/10.1016/j.compstruct.2019.01.105

[15] A. Z.M. Rahi, A. N. Al-Khazraji, A. A. Shandookh, Mechanical properties investigation of composite FGM fabricated from Al/Zn, Open Eng., 12 (2022) 789–798. https://doi.org/10.1515/eng-2022-0347

[16] I. Astm, ASTM E8/E8M-16a: Standard Test Methods for Tension Testing of Metallic Materials, West Conshohocken, PA, USA ASTM Int., 2016.

[17] W. D. Callister, D. G. Rethwisch, Mater. Sci. Eng. A., 7 (2007) John. Wiley . sons New York,

[18] E. ASTM, 606–80 Constant-Amplitude Low-Cycle Fatigue Testing Annual Book of ASTM Standards, Section, 3 (1986) 656–673.

[19] Z. M. R. Al-Hadrayi, A. N. Al-Khazraji, A. A. Shandookh, Investigation of Fatigue Behavior for Al/Zn Functionally Graded Material, Mater. Sci. Forum., 1079 (2022) 49–56. https://doi.org/10.4028/p-8umjsp